RILEM Technical Letters (2023) 8: 79-93
https://doi.org/10.21809/rilemtechlett.2023.178

Thermal conductivity of porous building materials: An exploration of new challenges in fractal modeling solutions

Marta Cappai[1], Giorgio Pia[1]*

[1] Dipartimento di Ingegneria Meccanica, Chimica e dei Materiali, Università degli Studi di Cagliari, Cagliari, Italy

Received: 23 May 2023 / Accepted: 25 September 2023 / Published online: 23 November 2023

Abstract

The improvement in the insulation material performance is one of the recent crucial problems. The energy consumption in the construction and buildings field has a significant impact on the society and the environment. For these reasons, researchers have focused on studying their thermal behaviour in order to improve fabrication methods and material design structures. In this sense, a great contribution has been offered by the modeling procedures. A remarkable attention has been dedicated to the application of fractal geometry which seems to be a promising method to replicate the porous structures as well as to predict the effective thermal conductivity. In this paper, a review of different modeling procedures is presented, comparing both traditional and fractal theory-based approaches. Fractal models demonstrate high reliability in reproducing experimental data under various conditions, including dry and moist systems. This is further enhanced by the application of recursive formulas, which streamline calculations even for complex porous microstructures. The choice between one model and another depends on the specific characteristics of the materials under study. In all cases, the versatility of the analytical procedures enables one to achieve a remarkable agreement with experimental data.

Keywords: Fractal geometry; Heat transfer; Modeling; Porous building materials; Thermal conductivity

1 Introduction

Energy consumption in the construction materials is a crucial point for this field [1–4]. Their constant growth is ascribable to different factors such as the increase in the world population and the improvement of the life-style standard in the residential or workplace buildings [5–7]. In EU, 40% of the energy is consumed by buildings which are also responsible for the 36% greenhouse gas emissions [8–12]. In addition to construction, renovation and demolition, a large quantity of this energy is dedicated to everyday use, especially for heating and cooling rooms and spaces. Indeed, the thermal management strongly influences the environment pollution, economic strategies and living standards [13–15]. This situation is made more complex by global geopolitical crisis which increases the cost of energy and the environmental safeguard target which promises to decrease the emissions of greenhouse gases [16]. As an example, comparing the first half of 2021 and 2022, average electricity and gas prices increased brusquely from 22.0 € to 25.3 € per 100 kWh and from 6.4 € to 8.6 € per 100 kWh respectively. The largest increase in the electricity price has been recorded in: Czechia +62%; Latvia +59%; and Denmark +57%, while the greatest increase in gas price is registered in: Estonia +154%; Lithuania +110%; and Bulgaria +108% [16]. Although the price of energy is currently decreased, it mainly depends on the decision of EU Member States to reduce the tax burden. This clearly helps us understand how fragile the structure is. Additionally, this system is subject to significant fluctuations that have an immediate impact on society [16].

At the same time, the lifestyle and environmental comfort require an increasingly higher energy consumption that hinders the fight against greenhouse gas emissions and climate change. In spite of the constant efforts, a step forward has still to be taken to achieve zero-emissions of greenhouse gases by 2050 as recommended by European Green Deal which has the ambition to transform Europe into a modern, energy and resource-efficient and economically competitive continent [8–12].

After these premises, the importance of the construction materials sector becomes evident from an energy perspective, both in terms of their production and implementation, as well as the actual savings resulting from their improved insulation performance. In this regard, it is clear that research interest is focusing on the development of innovative materials with modified structures, through the study of raw material mix design and manufacturing processes, to achieve superior thermal characteristics. An example of this is represented by binderless cotton stalk fiberboard aerogels, vacuum insulation panels, sustainable porous-insulation concrete, thermal insulation plasters, polystyrene-date palm, high-performance wood, phase change materials [17–22].

*Corresponding authors: Giorgio Pia, e-mail: giorgio.pia@unica.it

However, the complex production process leads to high costs, thus limiting their widespread utilization. Additionally, due to their limited mechanical strength, these systems can only be used in conjunction with structural materials, which often diminishes their performance [23].

It is imperative to highlight that significant results could be achieved via the improvement of construction materials' performance since they heavily influence the consumption of a considerable amount of energy [24–27]. For this reason, scientific research has laid emphasis on improving the energy efficiency and integration, technological development, industrial symbiosis, sustainability and durability besides paying a special attention to porous materials [23,27–31].

They are used in different fields such as industrial and engineering sectors with different applications in which porosity plays an important role; to influence heat transfer [32]. This complex aspect is regulated differently in the steady state and transient situations respectively by materials' thermal conductivity and a combination of thermal conductivity and specific heat capacity [32].

In general, the air trapped in the pores has a lower thermal conductivity as compared to the solid phase [33–35]. For this, porosity makes heat transfer difficult and consequently it influences the effective thermal conductivity of porous materials, resulting in lower than equivalent in bulk version. Moreover, the pore fraction (ε) is only an aspect of porosity capable of altering material's thermal conductivity. Other features are represented by pore size range, pore size distribution, pore capillary tortuosity, microstructure morphology and topology [36–39].

On one hand, traditional building materials are largely porous (rocks, ceramics, mortars and concretes). On the other hand, the fraction of voids, the morphology of the structures, the tortuosity of the capillaries etc. are intrinsic aspects of the materials and result from the production processes as they are. For this reason, greater control of porosity through the design of microscopic structures can lead to improved thermal insulation performance [36–39].

In this sense, the research in materials science and technology fields is constantly investigating the relationship between structure and thermal properties. A step forward is represented by different modeling approaches which can facilitate the comprehension of physical phenomena and improve material performances by new design strategies for fabricating porous material topologies [40–43].

In particular, over the last decades, fractal geometry has been used to construct models aimed at predicting thermal behaviour of different porous materials [44–46]. Based on self-similar geometry and recursive algorithms, they represent an intriguing challenge to represent the morphology of porous materials as well as to set up new simplified analytical procedures for calculating effective thermal conductivity.

Traditional models and new fractal modeling have been considered for studying heat transfer in porous systems. Calculations have been compared with experimental data in order to highlight their reliability and peculiarity.

2 Traditional models

Relevant studies have been carried out in order to predict thermal behaviour of porous materials, resulting in a great number of analytical models capable of calculating the effective thermal conductivity. Many of these are formalised for specific systems and their reliability is related to given materials. Often their generalisation is applicable by using empirical parameters.

However, other models are reference points for studying heat transfer in porous media and they present analytical formulas in function of solid and fluid thermal conductivity (k_s, k_f) values and density (φ) or pore fraction (ε).

The most used are represented by:

- Parallel and series models [47]

$$k_{parallel} = \varphi k_s + (1-\varphi)k_f \quad (1)$$

$$k_{series} = \frac{1}{\frac{(1-\varphi)}{k_f} + \frac{\varphi}{k_s}} \quad (2)$$

- Hashin and Shtrikman bounds [48]

$$k_{ME1} = k_f \frac{2k_f + k_s - 2(k_f - k_s)\varphi}{2k_f + k_s + (k_f + k_s)\varphi} \quad (3)$$

$$k_{ME2} = k_s \frac{2k_s + k_f - (k_s - k_f)(1-\varphi)}{2k_s + k_f + (k_s - k_f)(1-\varphi)} \quad (4)$$

- The EMT equation (proposed by Carson et al. [49])

$$k_{EMT} = \frac{[3\varphi - 1]k_s + [3(1-\varphi) - 1]k_f + \sqrt{\{[3\varphi - 1]k_s + [3(1-\varphi) - 1]k_f\}^2 + 8k_f k_s}}{4} \quad (5)$$

- The Ashby model [50], developed especially for solids with high porosity such as foams and lattices

$$k_{Ashby} = \frac{1}{3}\left[(1-\varepsilon) + 2(1-\varepsilon)^{2/3}\right]k_s + \varepsilon k_f \quad (6)$$

- The Krupiczka model [51], designed for the study of packed beds of spherical particles

$$k_e = k_f \left(\frac{k_s}{k_f}\right)^{0.28 - 0.757 \log \varepsilon - 0.057 \log\left(k_s/k_f\right)} \quad (7)$$

- The Revil model [52] elaborated for unconsolidated sediments

$$k_e = \frac{k_f}{f}\left[f\frac{k_s}{k_f} + 0.5\left(1-\frac{k_s}{k_f}\right)\left(1-\frac{k_s}{k_f}+\sqrt{\left(1-\frac{k_s}{k_f}\right)^2+4f\frac{k_s}{k_f}}\right)\right], f = \varepsilon^{\frac{m}{1-m}} \quad (8)$$

Where m is the cementation exponent equal to m=1/(1-L) and L is the depolarization factor [53].

In order to compare the calculations with experimental data presented in literature, dimensionless thermal conductivity, obtained by models, is calculated as

$$k_{mod}^{+} = \frac{k_{mod}}{k_f} \quad (9)$$

In Fig. 1 and 2, a comparison between experimental data obtained by literature (Ma et al. [54], Goual et al. [55], Jin et al. [56] and Shen et al. [57]) and traditional model calculations has been made. In particular, it is possible to see that experimental data only partially agree with predictions. Moreover, it is evident that the selection of the most appropriate model to be used is not pre-determinable. This fact becomes even more important while considering the significant variations in the range of predictions calculated by different models. For this reason, researchers have focused on developing generalisable models characterised by greater versatility in relation to the materials' structures.

An intriguing challenge is represented by the application of fractal geometry to obtain analytical procedures for calculating thermal conductivity.

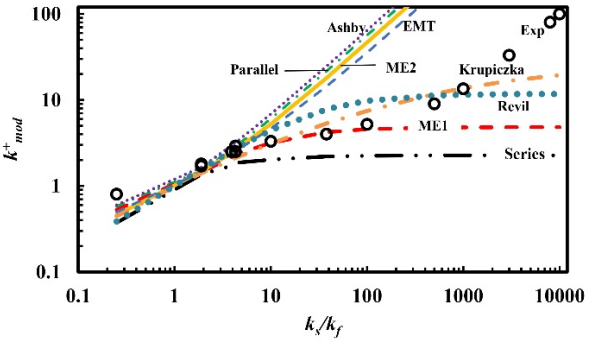

Figure 1. Comparison between experimental data reported in Ma et al. [54] and models trends: series, ME1, EMT, ME2, parallel, Ashby, Krupiczka and Revil.

3 What is a fractal geometry?

For porous materials, including building materials, there are different analytical and numerical procedures [18–24] for obtaining theoretical calculation of thermal conductivity. At present, a novelty is represented by the focus of this review, the application of fractal geometry to materials' microstructure [58]. For this, an introduction to fractal geometry is necessary.

Euclidian geometry is based on regular figures which are not capable of describing the shapes of nature. It is easy to recognise that "*Clouds are not spheres, mountains are not cones, coastlines are not circles and bark is not smooth, nor does lightning travel in a straight line…*" [59]. Indeed, all these and many other systems in nature are irregular and fragmented and exhibit a high degree of complexity that repeats itself at various observation scales.

Consequently, for studying and understanding, the intricate natural sets and phenomena need to be represented by a more realistic geometry. According to Maldelbrot, a relevant response arrives from Fractal geometry, formalised in 1975, which has been applied in a remarkable number of different fields. It is based on geometrical figure called *fractals* (from the Latin *fractus*: broken, jagged etc.; synonyms of *irregularity*) which have specific characteristics [59]. The most important is certainly the different concept of dimension. Contrary to Euclidian geometry in which dimensions are integer, fractals can have a fractional dimension. Moreover, fractals are obtained by iterative process, have an intricate and self-similar structure over a wide dimensional range and are not easily describable with traditional geometrical or analytical methods. The Sierpinski carpet is a well-known example of fractal figure (Fig.3a).

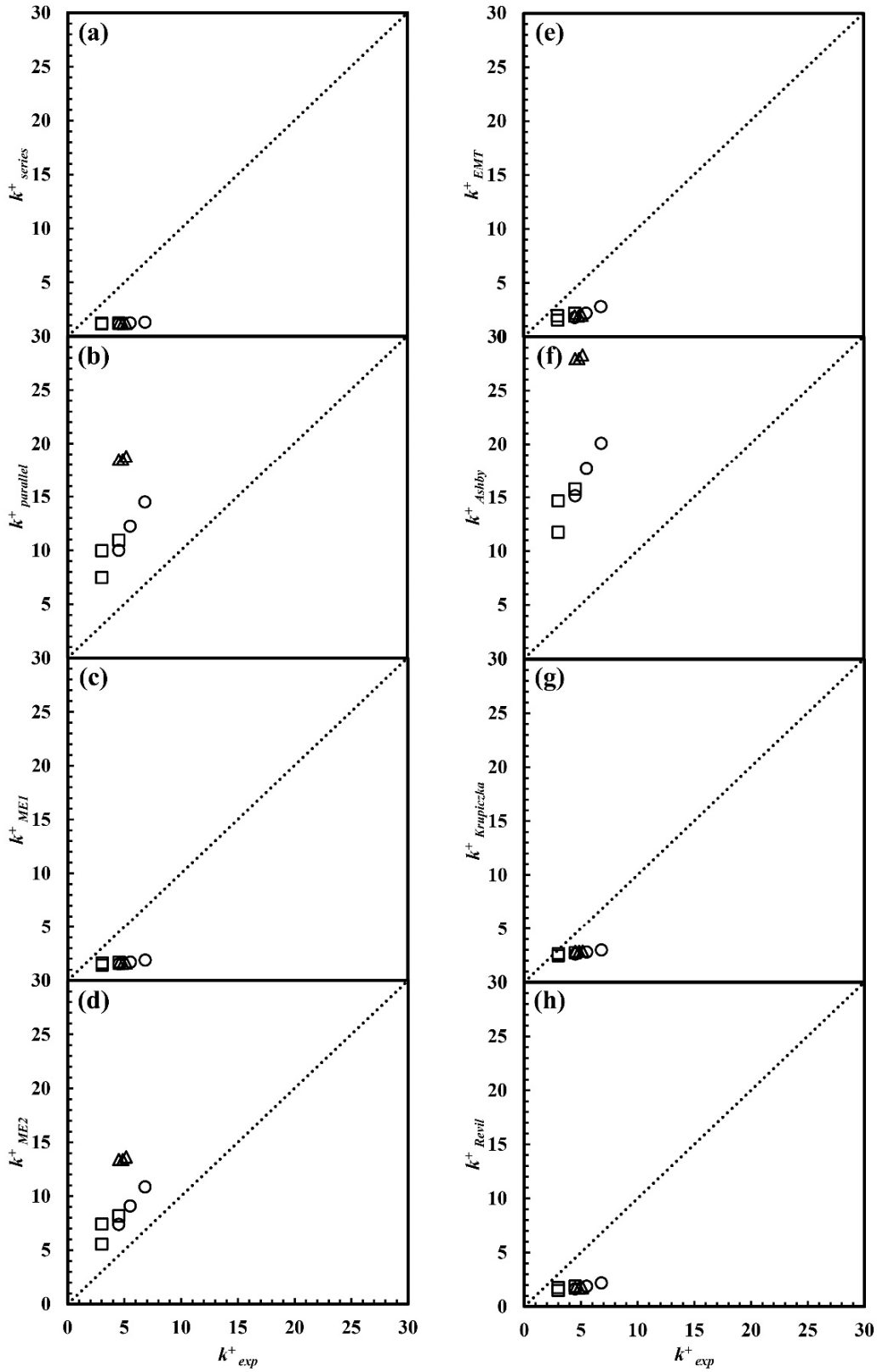

Figure 2. Comparison between experimental data reported in Goual et al. [55] (△), Jin et al. [56] (○), Shen et al. [57] (□) and models prediction: (a) series, (b) parallel, (c) ME1, (d) ME2, (e) EMT, (f) Ashby, (g) Krupiczka, (h) Revil. The dot line represents the perfect correlation between experimental and model data.

All these features are typical of deterministic fractals which are constructed by using a specific procedure (Fig.3a). However, it is also possible to obtain non-deterministic fractal (random fractal) aimed at representing more realistic phenomena (Fig. 3b).

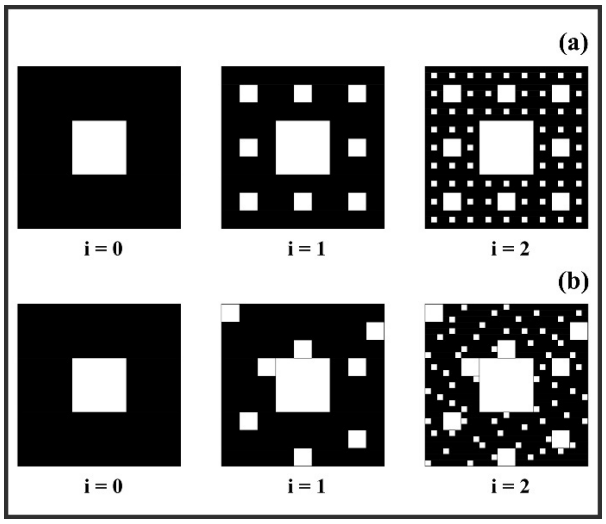

Figure 3. Deterministic (a) and randomised (b) Sierpinski carpet.

4 General application of fractal geometry during last two decades

Fractal geometry is applied in several areas such as mathematics, urban grow description, medical diagnoses, image compression and resolution, high performance multi-band device design, art, economy and materials science [59,60].

In the materials science, fractal modeling is used to represent microstructure as well as to formalise analytical expression aimed at understanding or predicting physical phenomena [59,60]. This is highlighted by a relevant and growing number of papers published based on fractal issues in materials science and engineering during the last 20 years (Fig.4).

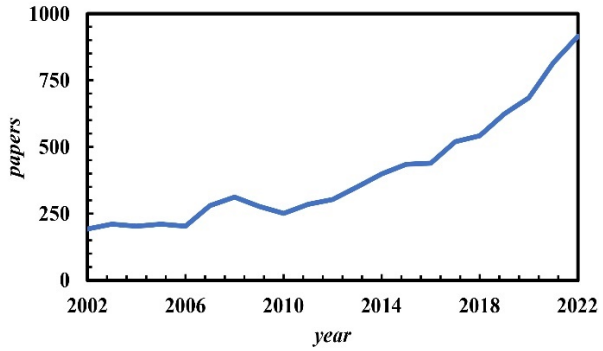

Figure 4. Papers published during last 20 years in which fractal modeling are presented for understanding physical phenomena. Data are acquired using Scopus.

The porous materials, their structure (pore fraction, pore size range, pore size distribution, capillary tortuosity and specific surface) and relative properties deserve a significative application. Some studies are reported as an example.

Xu et al. carried out a study to highlight how the morphology of soils influences water percolation into the pore structure arrangement. The calculations done by fractal function result in good agreement with experimental ones [61]. Wei et al. proposed the Cayley fractal tree model to describe the formation of chainlike silver nanostructure synthesised via a simple solvothermal process [62]. Pyun et al. investigated fractal features of mesoporous electrodes obtained by imprinting mesophase pitch which are used as a carbonaceous precursor and present diverse colloidal silica particles. It has been shown that fractal dimension can give data about porous structure. Specifically, fractal dimension (acquired by TEM micrographics image analysis) decreases when carbon specimen pores agglomerate [63]. Arandigoyen et al. focused their attention on the study of cement-lime mortars pore structure and mechanical properties by considering pore volume fraction, pore size distribution and fractal dimension [64,65]. Atzeni et al. calculated fractal dimensions of vesicular basalts and used these values such as specific parameter in a fuzzy model for obtaining mechanical properties classification [66]. Patra et al. observed porous microstructure evolution during sintering process of porous titania, highlighting a primary fractal structure which gradually lost with increase of temperature [67]. Sanyal et al. described the dendritic network in alloy solidification by using fractal geometry. The proposed fractal model has been capable of calculating effective permeability values of a lead-tin alloy fitting very well the experimental data [68]. Yu et al. carried out a deep study on the relationships between porous features and mass transfer by formalising new fractal models. Comparison between experimental and calculated data is in good agreement [69–74]. Tang et al. fabricated specimens based on stainless steel powder with recursive features. They observed a gradual increase in fractal dimension when porosity increases and proposed an analytical expression capable of correlating fractal dimension, porosity and magnification [75]. Buiting et Al. formalised a fractal tubular bundle model, in which pore sizes (diameters) are related to their lengths for calculating permeability of limestones [76]. In addition to phenomenological description of porous structures, fluid flow and mechanical properties, a great attention has been paid to understand heat transfer by using fractal concepts. Pia and Sanna proposed an intermingled fractal units model for studying the effect of materials topology on thermal conductivity [77–79]. Miao et al. proposed a model for calculating axially effective thermal conductivity in saturated dual porosity systems. It has been found that heat transfer is function of morphological characteristics such as pore volume fraction, pore tortuosity, fractal dimension of matrix, fractal orientation and thermal materials properties. Generally, the increase in effective thermal conductivity is related to the increase in ratio between thermal conductivity of solid and fluid phase (k_s/k_f) [80]. Deng et al. presented a fractal model for studying melting behaviours in metal foams. The approach allows to

find that porous media characterised by lower fractal dimensions facilitate melting heat transfer [81]. Wang et al. proposed a fractal procedure to describe thermal behaviour of moist porous building materials in which the coexistence of solid-liquid-gas thermal conductivity and capillary structure is taken into account. They found that thermal conductivity increases when saturation of media increases and fractal dimension of tortuosity and fractal dimension decrease [82]. Qin et al. proposed a new fractal model for saturated and unsaturated engineering materials. The calculation of the analytical expressions shows a great capacity to reproduce effective thermal conductivity experimental data in different conditions [83,84]. Yu et al. proposed a work in which full-scale Rosseland diffusion equation and fractal thermal modeling are combined. By considering a large quantity of aspects such as cell size, pore shape, specific surface area, pore volume fraction, temperature, refractive index etc., they formalised an analytical procedure aimed at representing experimental results. In particular, the obtained data made evident that thermal conductivity decreases when extinction index, structure volume and specific surface increases, while it decreases when temperature increases [85].

One aspect still debated is inherent in calculating the fractal dimension of porous systems. In this regard, Wood [86] published a paper in which he compares different methods for obtaining the fractal dimension. The common data sources are the isotherms obtained from gas adsorption experiments. The methods presented are Frenkel-Halsey-Hill (FHH), Neimark (NM), and Wang and Li (WL), along with their respective equations [86].

The FHH model [86,87] is based on the proportionality between the layer of gas adsorbed on the pore surfaces and the fractal dimension of these surfaces. This correlation is tested at different relative pressures as a part of the isotherm.

$$\ln N = a + (D - 3)\ln(-\ln X) \tag{10}$$

Where *N* is the volume of adsorbate adsorbed by the sample, *a* is a constant, *D* is the fractal dimension, and *X* is equal to the ratio P/P_0, a dimensionless relative pressure. This ratio represents the equilibrium pressure (*P*) of the porous sample for each pressure increment measured as part of the isotherm divided by the saturation pressure of nitrogen at 77 K (P_0).

The scatter plot developed, considering ln*N* vs ln(-ln*X*), allows the fractal dimension *D* to be identified by adding the slope of the line to the value 3.

The NM [86,88] model allows to calculate the fractal dimension from Eq. 11

$$\ln S = k - (D - 2)\ln r \tag{11}$$

Where *k* is a constant, *S* is the relates the surface area and is obtained by using the Kiselev relationship, and the pore radius *r* is determined through Kelvin's relationship [86].

Both relationships (Kiselev and Kelvin) can be solved by considering the slope and exponent of the best-fit curve obtained from the N vs. lnX graph, obtaining S and r, respectively [86].

By examining the ln*S* vs. ln*r* plot, *D* is determined by subtracting the negative slope of the best linear fit for that line from 2.

The WL [86,89] model enables the calculation of the fractal dimension using Eq. 12

$$\ln A(X) = l + D\ln B\,(X) \tag{12}$$

D is the slope of the equation of a line expressed in Eq. 12, *l* is constant, and A and B are equal to:

$$A(X) = \frac{-\int_{N(X)}^{N_{max}} \ln X dN(X)}{r^2(X)} \tag{13}$$

$$B(X) = \frac{[N_{max} - N(X)]^{\frac{1}{3}}}{r(X)} \tag{14}$$

Eqs. 13 and 14 can be solved, as in the NM technique, by the Kiselev and Kelvin relations.

5 Fractal models for predicting thermal conductivity

In this review, different fractal models are reported in order to show the relationships between structures and thermal behaviour in porous materials. The choice to present the following models allows us to highlight the versatility of formal analytical procedures through the use of fractal geometry. Models proposed below, starting from similar geometrical construction, can be generalised for different microstructures of materials and various conditions in which they may be found.

5.1 A self-similarity model for effective thermal conductivity of porous media by Ma et al.

A relevant study on the effective thermal conductivity of granular and composite materials or composed by sphere dispersed cells was conducted by Ma et al. [54]. Their analytical procedure was based on the fact that porous materials have fractal features and recursive structures. Statistical methods and iteration process were developed for describing thermal behaviour of porous media. Sierpinski carpet and its variations such as geometrical base unit and as schematic pattern for thermal-electrical analogy technique were used (Fig. 5).

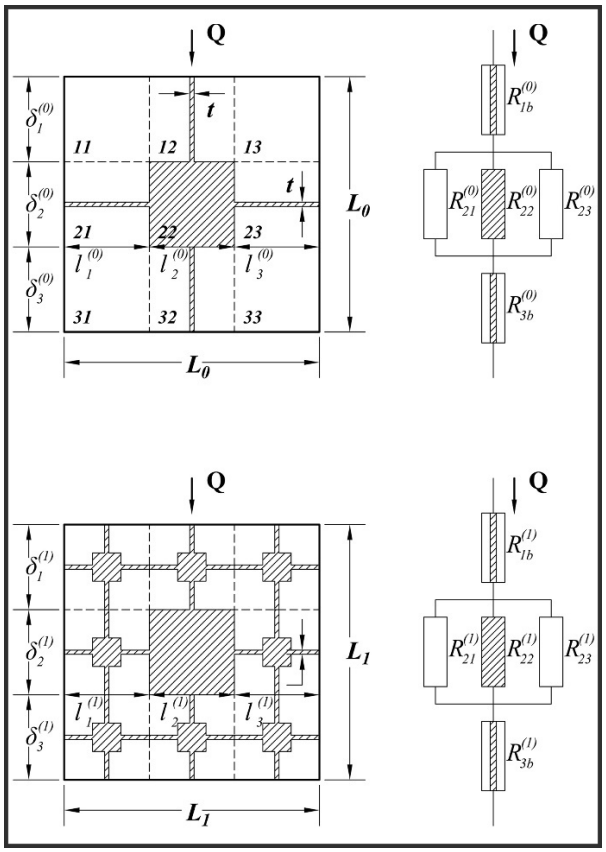

Figure 5. Self-similar model and thermal-electrical analogy pattern for predicting thermal conductivity. (a) 0-stage, (b) 1-stage.

In particular, this model considered the material structure composed by two different parts: one characterised by a random system of dispersed non-touching particles and another characterised by touching particles which are symmetrically distributed and have a thermal resistance.

The analytical formula, in which all terms have physical meaning, is expressed as a function of pore fraction, the ratio between non-touching particles area and total area of a representative cross section, the ratio between thermal conductivity of solid phase and thermal conductivity of matrix and the thermal resistance (Appendix 1).

$$k_{e,sc}^{+(n)} = \frac{3k_{e,sc}^{+(n-1)}}{2/\left[t^{+}\beta^{(n)}+(1-t^{+})\right]+1/\left(2/3+\beta^{(n)}/3\right)} \quad (15)$$

$$k_e^{+} = \frac{A_{nt}}{A}\left[\left(1-\sqrt{1-\varepsilon}\right)+\frac{\sqrt{1-\varepsilon}}{1+(1/\beta-1)\sqrt{1-\varepsilon}}\right]+\left(1-\frac{A_{nt}}{A}\right)k_{e,sc}^{+(n)} \quad (16)$$

Parametric elaborations are reported in Fig. 6a. Parametric calculations show that the contact resistance between particles is negligible when the ratio between thermal conductivity of solid phase and thermal conductivity of matrix or fluid (in this case $k_s/k_f = \beta$) is $\beta < 100$ [54].

A comparison between experimental data, reported in Ma et al. [54], and model predictions have been performed (Fig. 6b). The system is composed by materials with ε = 0.44. Unlike what is shown in Fig. 1, where traditional models only partially fit the experimental data (the best fit is obtained by comparing ME1 model), in the case of Ma et al.'s model, the correlation is in excellent agreement with the measured values across the entire range of k_s/k_f.

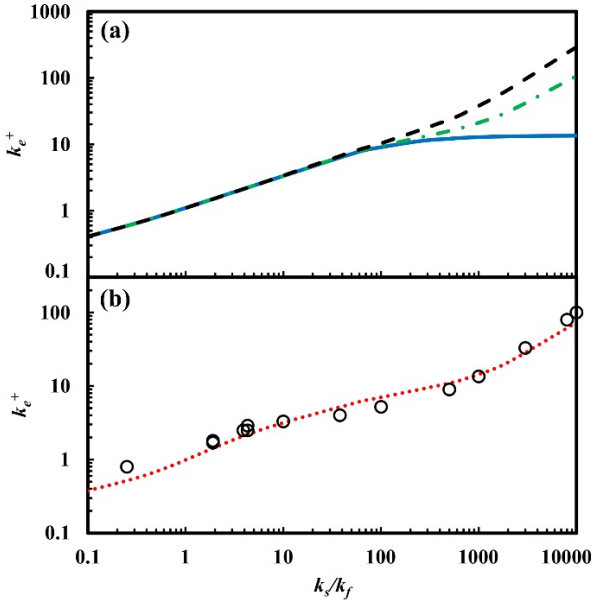

Figure 6. (a) Longitudinal contact resistance influence on the thermal conductivity. Calculations are performed for ε = 0.39; - t = 0 (—), t = 0.001 (– –) - t = 0.003 (– –). (b) Comparison between experimental data (○) reported in Ma et al. [54] and calculation performed by using their model (•••), ε = 0.44.

Further data are presented in the original paper [54]. It is evident that best fit is recorded especially for the cases in which β is greater than 1. When β is smaller than 1, model data are in better agreement with experimental ones [90,91].

5.2 Experimental determination and fractal modeling of the effective thermal conductivity of autoclaved aerated concrete: Effects of moisture content by Jin et al.

Jin et al. proposed a fractal model capable of predicting thermal conductivity in autoclaved aerated concrete [56]. These materials represent a promising choice in insulation and recently they attracted a remarkable attention for improving building thermal properties. The highest porosity of the considered samples is between 76% and 84%, consequently heat transfer into the structure is reduced. From mercury intrusion porosimetry tests and image analysis (reported in the paper), it is possible to note that pore range is between 400μm and 0.004 μm with two peaks around 100μm and 0.03 μm.

In this work, thermal conductivity experimental data are compared with model calculations based on fractal structures and electrical equivalence. The model is constructed on Sierpinski carpet and the geometry is similar to those proposed by Ma et al. [54] for dry state (Fig. 7a) and for the case in which moisture is present (Fig. 7b).

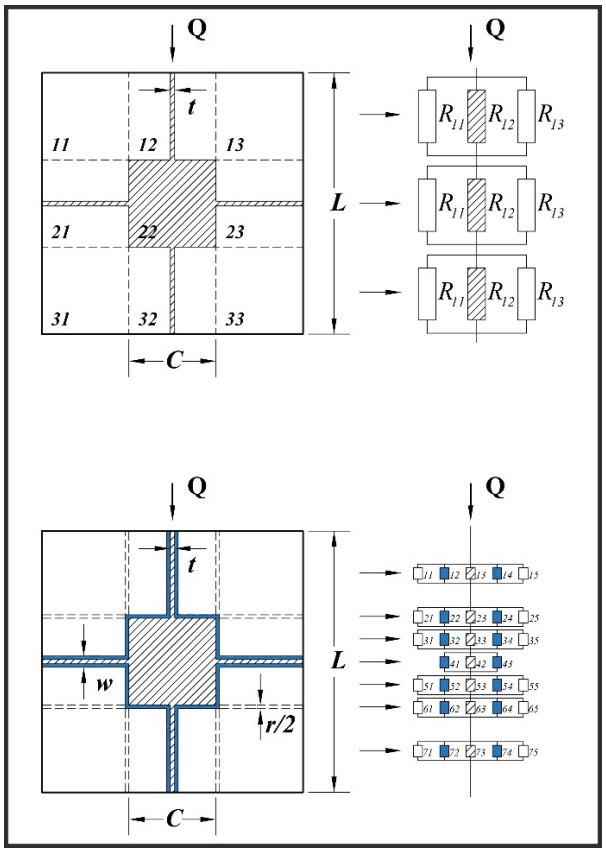

Figure 7. Self-similar model and thermal-electrical analogy pattern for predicting thermal conductivity. (a) structure at dry state, (b) structure with moisture content.

For the dry state, the analytical expressions for calculating the dimensionless thermal conductivity ($K^{(n)}$) and thermal conductivity (k^n) are reported in Eq. 17 and Eq. 18. Eq. 17 is a different way to express the Eq. 15 by Ma et al. (Appendix 2).

$$K^{(n)} = K^{(n-1)}\left[\frac{1-\alpha}{\tau(\kappa^{(n-1)}+1} + \frac{c}{C(\kappa^{(n-1)}-1)+L}\right]^{-1} \quad (17)$$

$$k^n = K^{(n)}k_a \quad (18)$$

Parametric calculations allow to show the variation of thermal conductivity in function of porosity for different τ ($\tau = t/L$) values. For the same value of porosity, when τ increases, k^n increases following the trends reported in Fig. 8a by using Eq. 18.

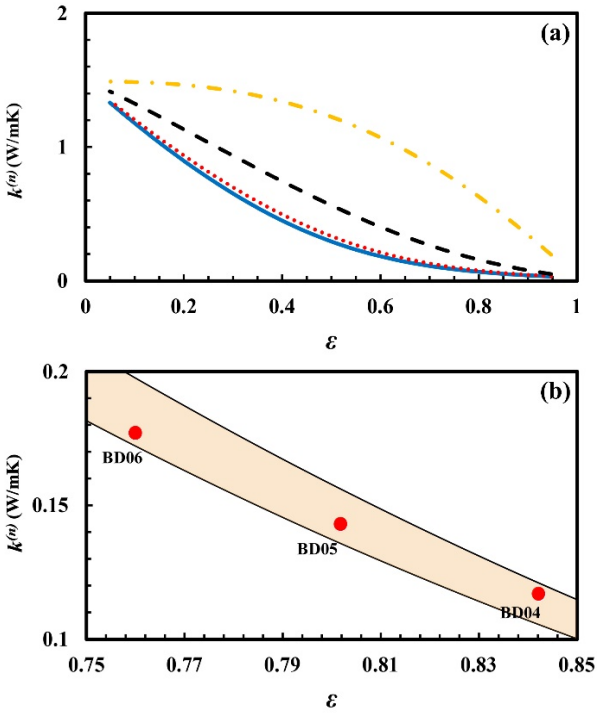

Figure 8. (a) parametric calculations of effective thermal conductivity vs pore fraction for C = 3; - τ = 0.00001 (—), - τ = 0.001 (•••), - τ = 0.01 (– –), - τ = 0.1 (– • –).; (b) Comparison between experimental data (●) and calculated data. Best fit curves (contained in the highlighted surface) are obtained for C=3, 0.0076< τ <0.01.

The reliability of the presented model has been verified for dry systems (in Jin et al. such as B04, B05 and B06) which are characterised respectively by a pore fraction equal to 0.84, 0.80 and 0.76 and a thermal conductivity equal to 0.117, 0.143 and 0.177 W/mK respectively.

Fig. 8b reports calculations for the best fit boundary conditions elaborated by using C = 3, L = 13 and τ between 0.0076 and 0.01. The highlighted area represents the infinite curves which can be obtained by varying τ in the selected range. It is evident that the model is in excellent agreement with experimental ones.

An effort has been made to describe thermal behaviour variations as a function of moisture presence. In this case, model construction is more complex and it is elaborated with three phases: matrix, water and air (Fig. 7b).

Analytical procedure is based on the development of Eq. 19 (Appendix 2) as a function of the Sierpinski carpet dimensions and lengths (which can be found in the structure), water content (from 0-100%) and thermal conductivity of the different phases (0.598 W/mK for water and 0.026 W/mK for air).

$$k = k_a\left[\frac{1-\alpha-\beta^{(n)}}{(1-\omega^{(n)}-\tau)+\kappa^{(n)}\tau+\kappa_w^{(n)}\omega^{(n)}} + \frac{\alpha-\omega^{(n)}}{(1-\alpha-\beta^{(n)})+\kappa^{(n)}\alpha+\kappa_w^{(n)}\beta^{(n)}} + \frac{\beta^{(n)}}{(1-\alpha-\beta^{(n)})+\kappa^{(n)}\tau+\kappa_w^{(n)}(1+\beta^{(n)}-\tau)} + \frac{\omega^{(n)}}{\kappa^{(n)}\alpha+\kappa_w^{(n)}(1-\alpha)}\right]^{-1} \quad (19)$$

As expected, thermal conductivity increases when moisture content increases and pore fraction decreases. The great versatility of the proposed model allows to find the proper configuration which offers the possibility to predict the experimental data carefully. Fig. 9 reports the experimental data and predictions published in [56]. The best fitting is obtained for moisture content between 15% and100%.

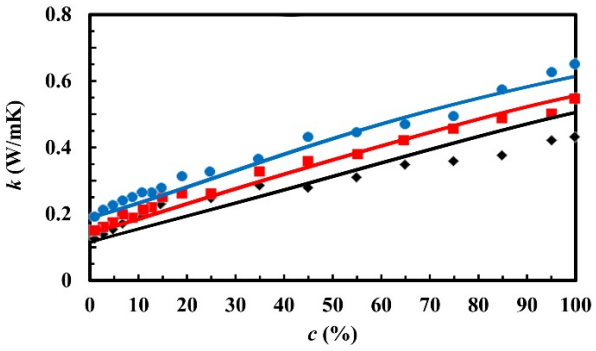

Figure 9. Thermal conductivity vs moisture content for B04 (◆), B05 (■) and B06(●). Experimental data and best fitting with C = 2 and τ = 0.003.

5.3 Analysis of axial thermal conductivity of dual-porosity fractal porous media with random fractures by Miao et al.

Miao et al. proposed a model to obtain the axial thermal conductivity for porous media characterised by a fractal porosity. In particular, this analytical procedure has been performed for dual-porosity systems which consist of a porous matrix and fractures randomly distributed. It deals with different fields of engineering applications in which natural materials (rocks, granular and vegetables) or artificial materials (metals and ceramics) are used. Geometrical composition considers a representative volume in which bundle of fractal tortuous capillaries and fractures are present (Fig. 10).

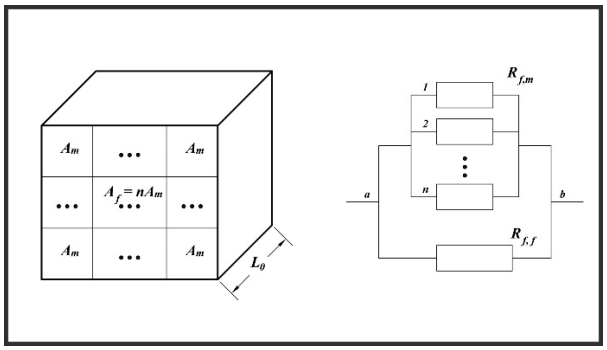

Figure 10. (a) Dual porosity model scheme and (b) relative thermal-electrical pattern.

The analytical procedure obtained is a function of microstructure characteristics such as the matrix and fracture porosities ($\mathcal{E}_m$, $\mathcal{E}_f$), fractal dimensions (D_f, D_l), tortuosity fractal dimension of pore capillaries (D_T), the orientation of fractures (dip ϑ, azimuth α) and thermal conductivity of solid and fluid phase (Appendix 3).

$$k_e = (1-\mathcal{E}_t)k_s + k_f\mathcal{E}_f\frac{1}{1-cos^2\alpha sin^2\theta} + k_f\mathcal{E}_m * \frac{\lambda_{max}^{D_T-1}}{L_0^{D_T-1}} * \frac{(2-D_f)\left[1-(\mathcal{E}_m)^{\frac{1+D_T-D_f}{2-D_f}}\right]}{(1-\mathcal{E}_m)(1+D_T-D_f)} \quad (20)$$

$$k^+ = \frac{k_e}{k_f} = (1-\mathcal{E}_t) * \frac{k_s}{k_f} + \mathcal{E}_f * \frac{1}{1-cos^2\alpha sin^2\theta} + \mathcal{E}_m * \frac{\lambda_{max}^{D_T-1}}{L_0^{D_T-1}} * \frac{(2-D_f)\left[1-(\mathcal{E}_m)^{\frac{1+D_T-D_f}{2-D_f}}\right]}{(1-\mathcal{E}_m)(1+D_T-D_f)} \quad (21)$$

The paper reports a parametric study for explaining the effect of different features on thermal conductivity. As reported in Fig. 11a, it is evident that when k_s/k_f increases, the effective thermal conductivity of dual porosity system increases. Comparing systems with different porosity, for k_s/k_f >1, thermal conductivity increases when porosity decreases, while for $k_s/k_f < 1$, the thermal conductivity increases when porosity increases [80].

A comparison between experimental values for fractured samples, developed by Surma et al. [92], and calculations performed by using l_{max} = 2cm, λ_{max} = 10^{-3} m, α = 0, ϑ = π/6 as input data shows a good agreement (Fig. 11b).

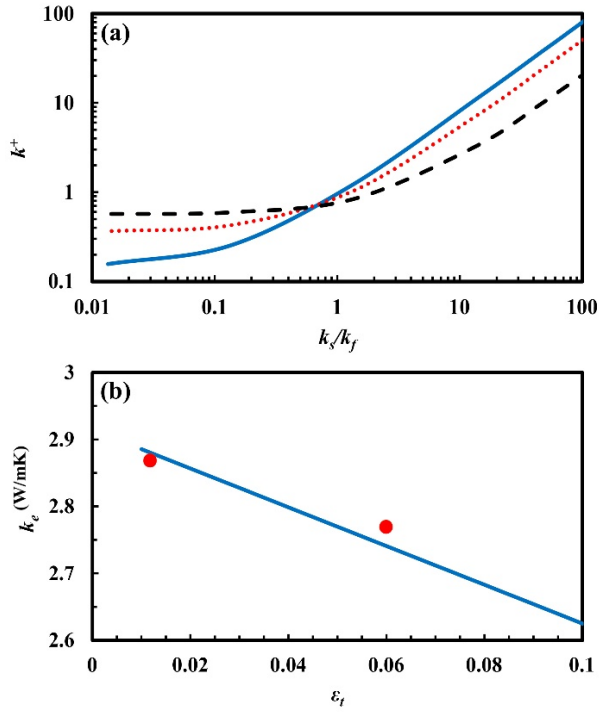

Figure 11. (a) The dimensionless effective thermal conductivity vs k_s/k_f at $\varepsilon_m/\varepsilon_f = 10$; $\varepsilon_t = 0.2$ (—), 0.5 (•••), 0.8 (– –). (b) Comparison between experimental by Surma et al. [92] and calculated data.

5.4 A generalized thermal conductivity model for unsaturated porous media with fractal geometry by Shen et al.

Shen et al. proposed a fractal generalised thermal conductivity model for unsaturated (partially saturated) porous materials in which three phases are present: gas, liquid and solid [57].

In this work, a new general fractal method which takes into account partially saturated porous structure features is suggested.

Indeed, the authors in their study highlighted that most medium- high porous materials have fractal porous structures mathematically represented by scaling laws in different scales. The geometrical set used is constructed by a fractal pore phase (as circles in cross sectional view) and non-fractal solid phase (homogeneous surface), Fig. 12.

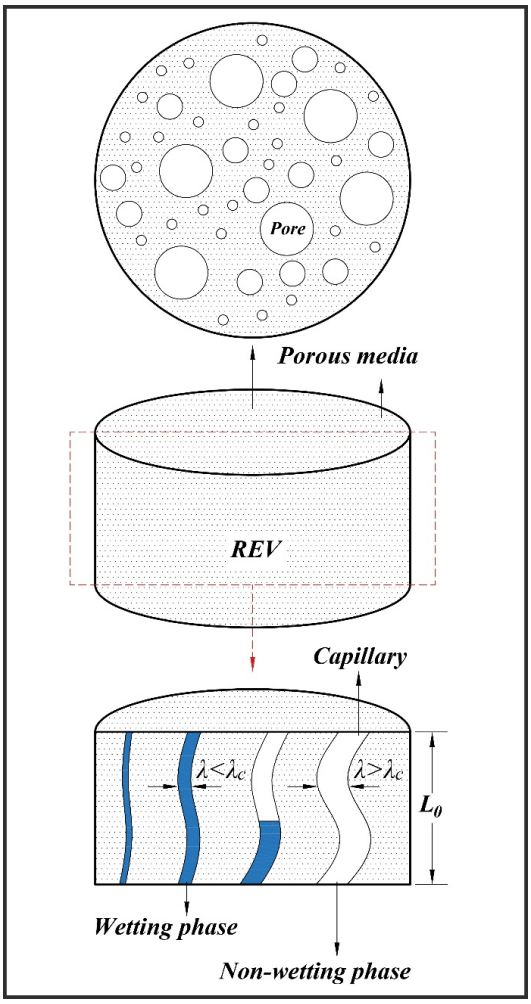

Figure 12. Model scheme for describing porous microstructure. REV: representative elementary volume.

Their model correlates thermal conductivity of gas, water and solid phases, i.e. k_g, k_w and k_s, the porosity (ε), pore and tortuosity fractal dimensions (D_f and D_T) and fluid phase saturation. The analytical procedure, which involves only physical quantities, results in (Appendix 4):

$$k^+ = \frac{(2-D_f)^{(D_T+1)/2}}{D_f^{(D_T-1)/2}(1+D_T-D_f)}\left(\frac{\varepsilon}{1-\varepsilon}\right)^{(D_T+1)/2} * \left\{1-[(1-\varepsilon)S_w+\varepsilon]^{\frac{1+D_T-D_f}{2-D_f}}\right\} + \frac{k_w}{k_g}\frac{(2-D_f)^{(D_T+1)/2}}{D_f^{(D_T-1)/2}(1+D_T-D_f)}\left(\frac{\varepsilon}{1-\varepsilon}\right)^{(D_T+1)/2} * \left\{[(1-\varepsilon)S_w+\varepsilon]^{\frac{1+D_T-D_f}{2-D_f}}\right\} + \frac{k_s}{k_g}(1-\varepsilon) \quad (22)$$

Parametric sensibility highlights the higher versatility of the model capable of covering the entire range of porosities and saturation, different pore size range in pore size distribution and different fractal pore and tortuosity dimensions.

In Fig. 13, it is possible to see the influence of porosity on the thermal conductivity for systems which have different saturation. In particular, Eq. 22 has been used taking into account D_f = 1.6, D_T = 1.1, $k_s/k_g = 170$, $k_w/k_g = 110$ and S_w equal to 0.2, 0.4, 0.6, 0.8 respectively. When porosity

increases, dimensionless effective thermal conductivity significantly decreases in relation to the decrease of solid phase. At the same time, dimensionless effective thermal conductivity increases when liquid saturation increases because $k_w > k_g$.

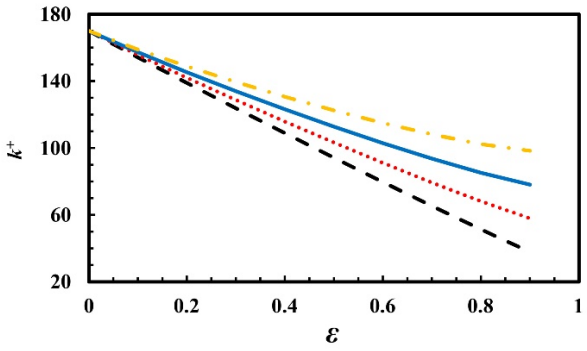

Figure 13. Porosity influence on effective thermal conductivity for different liquid saturation degrees. Sw is equal to 0.2 (– –), 0.4 (•••), 0.6 (—), 0.8 (– • –). Input data D_f = 1.6, D_T = 1.1, $k_s/k_g = 170$, $k_w/k_g = 110$.

Another parametric elaboration has been performed by considering pore fraction equal to 0.60, $k_s/k_g = 170$ and $k_w/k_g = 110$. In Fig. 14a, with D_T = 1.1, while changing the value of D_f , different curves are generated (D_f = 1.50, 1.60, 1.70, 1.80, 1.90). As expected, effective thermal conductivity increases when liquid saturation degree increases. Moreover, it is possible to note that D_f influences the effective thermal conductivity. Indeed, when D_f increases, k^+ decreases.

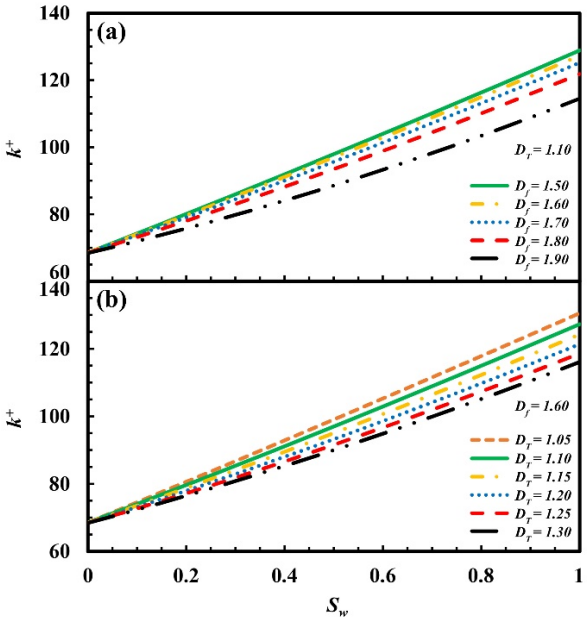

Figure 14. k+ vs Sw for different values of Df and DT. (a) D_T = 1.1; D_f = 1.50, 1.60, 1.70, 1.80, 1.90; $k_s/k_g = 170$, $k_w/k_g = 110$. (b) D_f = 1.60; D_T = 1.05, 1.10, 1.15, 1.20, 1.25, 1.30; $k_s/k_g = 170$, $k_w/k_g = 110$.

In Fig. 14b, with D_f = 1.6, while changing the value of D_T, different curves are generated (D_T = 1.05, 1.10, 1.15, 1.20, 1.25, 1.30). Effective thermal conductivity behaviour *vs* liquid saturation has the same trend of the previous case. Moreover, D_T also influences the effective thermal conductivity and when D_T increases, k^+ decreases. Thus, more complex structures have lower effective thermal conductivity.

The reliability of the model has been verified by comparing experimental data with calculations (Fig. 15). A good agreement has been found and the model seems to be adapted for general applications. As considered by the authors, additional improvements could be performed in future by considering bound and trapped liquid and series connection of wetting and non-wetting phases which were neglected at the moment. However, these considerations could greatly complicate the model which is, in this form, easily to use.

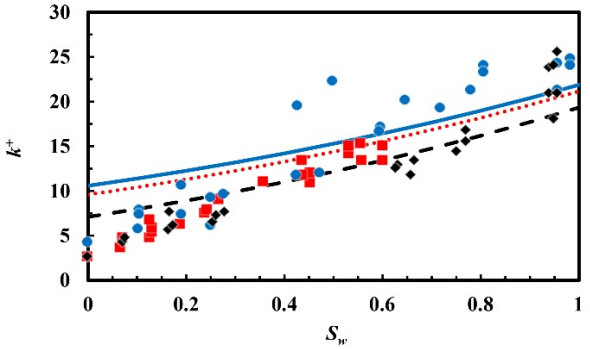

Figure 15. Comparison between experimental and calculation data [57]. Model curves have been obtained for systems with: ε = 0.87(– –), 0.82 (•••), 0.80 (—); D_T = 1.1; D_f = 1.980 (– –), 1.971 (•••), 1.967 (—), $k_s/k_g = 50.4$; $k_w/k_g = 23.1$.

6 Perspective, trends and conclusions

The use of fractal geometry for the formalisation of predictive models of thermal conductivity in porous materials has proven to be quite promising. The ability to simulate real microstructures through iterative procedures that exploit self-similarity properties is used as a powerful tool. The resulting analytical procedures based on recursive formulas allow for a significant simplification of calculations by resolving the schemes used at different scales without further levels of complexity.

The results obtained show an encouraging agreement with experimental data acquired through tests conducted in the laboratory. However, there is still considerable room for improvement. Currently, most published fractal models use simple geometries to reproduce real microstructures, which in some cases are very complex and articulate. The number of solid and fluid phases present in some cases is not reproducible with classical deterministic fractals. Therefore, further effort will be required in research and development of suitable geometries without losing the essential aspects already obtained.

Another important fact that needs to be considered is the scale effect on thermal properties. Fractal modeling is capable of replicating material structures across the entire range of porosity, but further research is needed to link dimensional variations to those of heat transfer.

In summary, the future prospects for the use of fractal geometry for the formalisation of predictive models of thermal conductivity in porous materials are definitely promising and require further research and development to overcome current challenges.

Acknowledgment

The financial support of Fondazione di Sardegna, project F72F20000360007 and of University of Cagliari are also gratefully acknowledged.

Authorship statement (CRediT)

Giorgio Pia: conceptualization; data curation; formal analysis; funding acquisition; investigation; methodology; project administration; resources; software; supervision; validation; visualization; writing – original draft; writing – review & editing.

Marta Cappai: conceptualization; data curation; formal analysis; funding acquisition; investigation; methodology; software; validation; visualization; writing – original draft; writing – review & editing.

Appendix 1. Nomenclature Ma et al.

k_e^+	Dimensionless effective thermal conductivity
A	Total area of representative cross section (m^2)
A_{nt}	Equivalent area of a cross section having the same porosity as the non-touching particles (m^2)
ε	pore fraction
β	ratio of thermal conductivity of solid and thermal conductivity of matrix
$k_{e,sc}^{+(n)}$	Dimensionless effective thermal conductivity for an n-stage carpet

Appendix 2. Nomenclature by Jin et al.

K	dimensionless thermal conductivity
k	thermal conductivity (W/mK)
k_a	thermal conductivity of dry air (W/mK)
L	side length of the Sierpinski carpet
C	side length of the central matrix
α	dimensionless side length of the central matrix, defined by C/L
τ	dimensionless width of virtual thermal resistances, defined by t/L
κ	ratio of matrix to dry air thermal conductivity
κ_w	ratio of matrix to water thermal conductivity
β	dimensionless thickness of surrounding water layer, defined by r/L
ω	dimensionless width of connected water bridges, defined by w/L
n	stage of Sierpinski carpet

Appendix 3. Nomenclature by Miao et al.

D_f	fractal dimension for pore area
D_T	fractal dimension for tortuosity
k_e	effective thermal conductivity of a dual-porosity medium (W/mK)
k_f	thermal conductivity of fluid in the capillary (W/mK)
k_s	thermal conductivity of solid matrix (W/mK)
k^+	dimensionless effective thermal conductivity
L_0	straight length of a tortuous capillary
α	the mean azimuth of fractures
λ_{max}	the maximum pore diameter
Θ	the mean dip angle of fractures
ε_f	pore fraction of a fracture network
ε_m	pore fraction of porous matrix
E_t	total pore fraction of a dual-porosity medium

Appendix 4.Nomenclature by Shen et al.

k^+	dimensionless thermal conductivity (W/mK)
D_f	fractal dimension
D_T	tortuosity dimension
S_w	wetting phase (liquid) saturation
k_w	thermal conductivity of solid phase (W/mK)
k_s	thermal conductivity of wetting phase (liquid) (W/mK)
k_g	thermal conductivity of non-wetting phase (gas) (W/mK)
ε	pore fraction

References

[1] S. Rashidi, J.A. Esfahani, N. Karimi, Porous materials in building energy technologies—A review of the applications, modelling and experiments, Renew. Sustain. Energy Rev. 91 (2018) 229–247. https://doi.org/10.1016/j.rser.2018.03.092

[2] L. Chen, Y. Zhao, R. Xie, B. Su, Y. Liu, X. Renfei, Embodied energy intensity of global high energy consumption industries: A case study of the construction industry, Energy. (2023) 127628. https://doi.org/10.1016/j.energy.2023.127628

[3] G. Shang, L. Xu, J. Tian, D. Cai, Z. Xu, Z. Zhou, A real-time green construction optimization strategy for engineering vessels considering fuel consumption and productivity: A case study on a cutter suction dredger, Energy. 274 (2023) 127326. https://doi.org/10.1016/j.energy.2023.127326

[4] S. Yu, H. Tang, D. Zhang, S. Wang, M. Qiu, G. Song, D. Fu, B. Hu, X. Wang, MXenes as emerging nanomaterials in water purification and environmental remediation, Sci. Total Environ. 811 (2022) 152280. https://doi.org/10.1016/j.scitotenv.2021.152280.

[5] X. Wei, R. Qiu, Y. Liang, Q. Liao, J.J. Klemeš, J. Xue, H. Zhang, Roadmap to carbon emissions neutral industrial parks: Energy, economic and environmental analysis, Energy. 238 (2022) 121732. https://doi.org/10.1016/j.energy.2021.121732.

[6] E. Alayed, D. Bensaid, R. O'Hegarty, O. Kinnane, Thermal mass impact on energy consumption for buildings in hot climates: A novel finite element modelling study comparing building constructions for arid climates in Saudi Arabia, Energy Build. 271 (2022) 112324. https://doi.org/10.1016/j.enbuild.2022.112324.

[7] J. Famiglietti, H.A. Toosi, A. Dénarié, M. Motta, Developing a new data-driven LCA tool at the urban scale: The case of the energy performance of the building sector, Energy Convers. Manag. 256 (2022) 115389. https://doi.org/10.1016/j.enconman.2022.115389.

[8] UNEP/Earthprint, U.N.E. Programme Buildings and Climate Change, (2007).

[9] E.E.C.D. E. Commission, EU buildings database - energy European commission, (2016).

[10] EU, Directive 2010/31/EU of the European Parliament and of the Council of 19 May 2010 on the energy performance of buildings (recast), Off. J. Eur. Union. (2010) 13–35. https://doi.org/doi:10.3000/17252555.L_2010.153.eng.

[11] E. Union, Directive 2012/27/EU of the European Parliament and of the Council of 25 October 2012 on Energy Efficiency, Amending Directives 2009/125/EC and 2010/30/EU and Repealing Directives 2004/8/EC and 2006/32/EC (Text with EEA Relevance), (2012).

[12] E. Union, Directive (EU) 2018/844 of the European Parliament and of the Council of 30 May 2018 Amending Directive 2010/31/EU on the Energy Performance of Buildings and Directive 2012/27/EU on Energy Efficiency, (2018).

[13] Y.K. Dwivedi, L. Hughes, A.K. Kar, A.M. Baabdullah, P. Grover, R. Abbas, D. Andreini, I. Abumoghli, Y. Barlette, D. Bunker, L. Chandra Kruse, I. Constantiou, R.M. Davison, R. De', R. Dubey, H. Fenby-Taylor, B. Gupta, W. He, M. Kodama, M. Mäntymäki, B. Metri, K. Michael, J. Olaisen, N. Panteli, S. Pekkola, R. Nishant, R. Raman, N.P. Rana, F. Rowe, S. Sarker, B. Scholtz, M. Sein, J.D. Shah, T.S.H. Teo, M.K. Tiwari, M.T. Vendelø, M. Wade, Climate change and COP26: Are digital technologies and information management part of the problem or the solution? An editorial reflection and call to action, Int. J. Inf. Manage. 63 (2022) 102456. https://doi.org/10.1016/j.ijinfomgt.2021.102456.

[14] D. Cheriyan, J. Choi, A review of research on particulate matter pollution in the construction industry, J. Clean. Prod. 254 (2020) 120077. https://doi.org/10.1016/j.jclepro.2020.120077.

[15] J.R. Zhao, R. Zheng, J. Tang, H.J. Sun, J. Wang, A mini-review on building insulation materials from perspective of plastic pollution: Current issues and natural fibres as a possible solution, J. Hazard. Mater. 438 (2022) 129449. https://doi.org/10.1016/j.jhazmat.2022.129449.

[16] Eurostat, Electricity & gas hit record prices in 2022, (2023).

[17] M. Zwerger, H. Klein, Integration of VIP's into external wall insulation systems, in: Proc. 7th Int. Vac. Insul. Symp., 2005: pp. 173–179.

[18] X. yan Zhou, F. Zheng, H. guan Li, C. long Lu, An environment-friendly thermal insulation material from cotton stalk fibers, Energy Build. 42 (2010) 1070–1074. https://doi.org/10.1016/j.enbuild.2010.01.020.

[19] A. Mariani, G. Malucelli, Transparent Wood-Based Materials: Current State-of-the-Art and Future Perspectives, 2022. https://doi.org/10.3390/ma15249069.

[20] L. Aditya, T.M.I. Mahlia, B. Rismanchi, H.M. Ng, M.H. Hasan, H.S.C. Metselaar, O. Muraza, H.B. Aditiya, A review on insulation materials for energy conservation in buildings, Renew. Sustain. Energy Rev. 73 (2017) 1352–1365. https://doi.org/10.1016/j.rser.2017.02.034.

[21] H. Yu, I. Zahidi, D. Liang, Sustainable porous-insulation concrete (SPIC) material: recycling aggregates from mine solid waste, white waste and construction waste, J. Mater. Res. Technol. 23 (2023) 5733–5745. https://doi.org/10.1016/j.jmrt.2023.02.181.

[22] A. Lachheb, A. Allouhi, M. El Marhoune, R. Saadani, T. Kousksou, A. Jamil, M. Rahmoune, O. Oussouaddi, Thermal insulation improvement in construction materials by adding spent coffee grounds: An experimental and simulation study, J. Clean. Prod. 209 (2019) 1411–1419. https://doi.org/10.1016/j.jclepro.2018.11.140.

[23] M.L. Qu, S.Q. Tian, L.W. Fan, Z.T. Yu, J. Ge, An experimental investigation and fractal modeling on the effective thermal conductivity of novel autoclaved aerated concrete (AAC)-based composites with silica aerogels (SA), Appl. Therm. Eng. 179 (2020) 115770. https://doi.org/10.1016/j.applthermaleng.2020.115770.

[24] A.M. Raimundo, A.M. Sousa, A.V.M. Oliveira, Assessment of Energy, Environmental and Economic Costs of Buildings' Thermal Insulation–Influence of Type of Use and Climate, Buildings. 13 (2023). https://doi.org/10.3390/buildings13020279.

[25] B. Petter Jelle, Nano-based thermal insulation for energy-efficient buildings, in: Start-Up Creat., Elsevier, 2016: pp. 129–181. https://doi.org/10.1016/B978-0-08-100546-0.00008-X.

[26] L. Long, H. Ye, The roles of thermal insulation and heat storage in the energy performance of the wall materials: A simulation study, Sci. Rep. 6 (2016) 1–9. https://doi.org/10.1038/srep24181.

[27] T. Li, M. Zhu, Z. Yang, J. Song, J. Dai, Y. Yao, W. Luo, G. Pastel, B. Yang, L. Hu, Wood Composite as an Energy Efficient Building Material: Guided Sunlight Transmittance and Effective Thermal Insulation, Adv. Energy Mater. 6 (2016). https://doi.org/10.1002/aenm.201601122.

[28] H. Gharibi, D. Mostofinejad, H. Bahmani, H. Hadadzadeh, Improving thermal and mechanical properties of concrete by using ceramic electrical insulator waste as aggregates, Constr. Build. Mater. 338 (2022) 127647. https://doi.org/10.1016/j.conbuildmat.2022.127647.

[29] L. Qiu, H. Zou, D. Tang, D. Wen, Y. Feng, X. Zhang, Inhomogeneity in pore size appreciably lowering thermal conductivity for porous thermal insulators, Appl. Therm. Eng. 130 (2018) 1004–1011. https://doi.org/10.1016/j.applthermaleng.2017.11.066.

[30] M.A. Mahmud, N. Abir, F.R. Anannya, A. Nabi Khan, A.N.M.M. Rahman, N. Jamine, Coir fiber as thermal insulator and its performance as reinforcing material in biocomposite production, Heliyon. 9 (2023) e15597. https://doi.org/10.1016/j.heliyon.2023.e15597.

[31] M.R. Hall, K.B. Najim, C.J. Hopfe, Transient thermal behaviour of crumb rubber-modified concrete and implications for thermal response and energy efficiency in buildings, Appl. Therm. Eng. 33–34 (2012) 77–85. https://doi.org/10.1016/j.applthermaleng.2011.09.015.

[32] I. Sumirat, Y. Ando, S. Shimamura, Theoretical consideration of the effect of porosity on thermal conductivity of porous materials, J. Porous Mater. 13 (2006) 439–443. https://doi.org/10.1007/s10934-006-8043-0.

[33] W.H. Khushefati, R. Demirboğa, K.Z. Farhan, Assessment of factors impacting thermal conductivity of cementitious composites—A review, Clean. Mater. 5 (2022) 100127. https://doi.org/10.1016/j.clema.2022.100127.

[34] Z. Fu, J. Corker, T. Papathanasiou, Y. Wang, Y. Zhou, O.A. Madyan, F. Liao, M. Fan, Critical review on the thermal conductivity modelling of silica aerogel composites, J. Build. Eng. 57 (2022) 104814. https://doi.org/10.1016/j.jobe.2022.104814.

[35] S. Chen, S. Ruan, Q. Zeng, Y. Liu, M. Zhang, Y. Tian, D. Yan, Pore structure of geopolymer materials and its correlations to engineering properties: A review, Constr. Build. Mater. 328 (2022) 127064. https://doi.org/10.1016/j.conbuildmat.2022.127064.

[36] I. Kaur, R.L. Mahajan, P. Singh, Generalized correlation for effective thermal conductivity of high porosity architectured materials and metal foams, Int. J. Heat Mass Transf. 200 (2023) 123512. https://doi.org/10.1016/j.ijheatmasstransfer.2022.123512.

[37] H. Liu, X. Zhao, Thermal Conductivity Analysis of High Porosity Structures with Open and Closed Pores, Int. J. Heat Mass Transf. 183 (2022) 122089. https://doi.org/10.1016/j.ijheatmasstransfer.2021.122089.

[38] Y.-J. Kim, B.-H. Park, S.-K. Hyun, H. Nishikawa, The influence of porosity and pore shape on the thermal conductivity of silver sintered joint for die attach, Mater. Today Commun. 29 (2021) 102772. https://doi.org/10.1016/j.mtcomm.2021.102772.

[39] J. Wang, Y. Chen, Y. Feng, G. Zhao, X. Jian, Q. Huang, L. Yang, J. Xu, Influence of porosity on anisotropic thermal conductivity of SiC fiber

reinforced SiC matrix composite: A microscopic modeling study, Ceram. Int. 46 (2020) 28693–28700. https://doi.org/10.1016/j.ceramint.2020.08.029.
[40] D. Șova, M.D. Stanciu, S.V. Georgescu, Design of Thermal Insulation Materials with Different Geometries of Channels, Polymers (Basel). 13 (2021) 2217. https://doi.org/10.3390/polym13132217.
[41] H. Gao, H. Liu, L. Liao, L. Mei, G. Lv, L. Liang, G. Zhu, Z. Wang, D. Huang, Improvement of performance of foam perlite thermal insulation material by the design of a triple-hierarchical porous structure, Energy Build. 200 (2019) 21–30. https://doi.org/10.1016/j.enbuild.2019.07.010.
[42] X. Wang, A. Li, X. Liu, X. Wan, Thermal Insulation and Compressive Performances of 3D Printing Flexible Load-Bearing and Thermal Insulation Integrated Lattice, Materials (Basel). 15 (2022). https://doi.org/10.3390/ma15238625.
[43] F. Anjum, M. Yasin Naz, A. Ghaffar, K. Kamran, S. Shukrullah, S. Ullah, Sustainable insulating porous building materials for energy-saving perspective: Stones to environmentally friendly bricks, Constr. Build. Mater. 318 (2022) 125930. https://doi.org/10.1016/j.conbuildmat.2021.125930.
[44] P. Yu, Y.H. Duan, E. Chen, S.W. Tang, X.R. Wang, Microstructure-based fractal models for heat and mass transport properties of cement paste, Int. J. Heat Mass Transf. 126 (2018) 432–447. https://doi.org/10.1016/j.ijheatmasstransfer.2018.05.150.
[45] G. Pia, C. Esposito Corcione, R. Striani, L. Casnedi, U. Sanna, Coating's influence on water vapour permeability of porous stones typically used in cultural heritage of Mediterranean area: Experimental tests and model controlling procedure, Prog. Org. Coatings. 102 (2017) 239–246. https://doi.org/10.1016/j.porgcoat.2016.10.021.
[46] Y.-L. He, T. Xie, Advances of thermal conductivity models of nanoscale silica aerogel insulation material, Appl. Therm. Eng. 81 (2015) 28–50. https://doi.org/10.1016/j.applthermaleng.2015.02.013.
[47] L. Gong, Y. Wang, X. Cheng, R. Zhang, H. Zhang, Thermal conductivity of highly porous mullite materials, Int. J. Heat Mass Transf. 67 (2013) 253–259. https://doi.org/10.1016/j.ijheatmasstransfer.2013.08.008.
[48] Z. Hashin, S. Shtrikman, A Variational Approach to the Theory of the Effective Magnetic Permeability of Multiphase Materials, J. Appl. Phys. 33 (1962) 3125. https://doi.org/10.1063/1.1728579.
[49] J.K. Carson, S.J. Lovatt, D.J. Tanner, A.C. Cleland, Thermal conductivity bounds for isotropic, porous materials, Int. J. Heat Mass Transf. 48 (2005) 2150–2158. https://doi.org/10.1016/j.ijheatmasstransfer.2004.12.032.
[50] M.F. Ashby, The properties of foams and lattices, Philos. Trans. R. Soc. A Math. Phys. Eng. Sci. 364 (2006) 15–30. https://doi.org/10.1098/rsta.2005.1678.
[51] R. Krupiczka, Analysis of thermal conductivity in granular materials, Int. Chem. Eng. 7(1) (1967) 122-+.
[52] A. Revil, Thermal conductivity of unconsolidated sediments with geophysical applications thermal conductivity • p In order to take into account for the thermal interactions between the, J. Geophys. Res. 105 (2000) 749–768. http://onlinelibrary.wiley.com/doi/10.1029/2000JB900043/full.
[53] P.N. Sen, M.H. Cohen, A self-similar model for sedimentary rocks with application to the dielectric constant of fused glass beads., Geophysics. 46 (1981) 781–795. https://doi.org/10.1190/1.1441215.
[54] Y. Ma, B. Yu, D. Zhang, M. Zou, A self-similarity model for effective thermal conductivity of porous media, J. Phys. D. Appl. Phys. 36 (2003) 2157–2164. https://doi.org/10.1088/0022-3727/36/17/321.
[55] M.S. Goual, A. Bali, M. Quéneudec, Effective thermal conductivity of clayey aerated concrete in the dry state: Experimental results and modelling, J. Phys. D. Appl. Phys. 32 (1999) 3041–3046. https://doi.org/10.1088/0022-3727/32/23/310.
[56] H.Q. Jin, X.L. Yao, L.W. Fan, X. Xu, Z.T. Yu, Experimental determination and fractal modeling of the effective thermal conductivity of autoclaved aerated concrete: Effects of moisture content, Int. J. Heat Mass Transf. 92 (2016) 589–602. https://doi.org/10.1016/j.ijheatmasstransfer.2015.08.103.
[57] Y. Shen, P. Xu, S. Qiu, B. Rao, B. Yu, A generalized thermal conductivity model for unsaturated porous media with fractal geometry, Int. J. Heat Mass Transf. 152 (2020) 119540. https://doi.org/10.1016/j.ijheatmasstransfer.2020.119540.
[58] W. Chen, Y. Wang, D. Wang, Y. Liu, J. Liu, Predicting the effective thermal conductivity of porous building materials using improved Menger sponge fractal structure, Int. J. Therm. Sci. 184 (2023) 107985. https://doi.org/10.1016/j.ijthermalsci.2022.107985.
[59] B.B. Mandelbrot, The Fractal Geometry of Nature, Freeman, New York, 2004.
[60] K. Falconer, Fractal Geometry: Mathematical Foundations and Applications, Wiley, New York, 2003.
[61] Y.F. Xu, D.A. Sun, A fractal model for soil pores and its application to determination of water permeability, Phys. A Stat. Mech. Its Appl. 316 (2002) 56–64. https://doi.org/10.1016/S0378-4371(02)01331-6.
[62] G.D. Wei, Y. Deng, C.W. Nan, Self-organized formation of chainlike silver nanostructure with fractal geometry, Chem. Phys. Lett. 367 (2003) 512–515. https://doi.org/10.1016/S0009-2614(02)01805-5.
[63] S. Il Pyun, C.K. Rhee, An investigation of fractal characteristics of mesoporous carbon electrodes with various pore structures, Electrochim. Acta. 49 (2004) 4171–4180. https://doi.org/10.1016/j.electacta.2004.04.012.
[64] M. Arandigoyen, J.I. Alvarez, Blended pastes of cement and lime: Pore structure and capillary porosity, Appl. Surf. Sci. 252 (2006) 8077–8085. https://doi.org/10.1016/j.apsusc.2005.10.019.
[65] M. Arandigoyen, J.I. Alvarez, Pore structure and mechanical properties of cement–lime mortars, Cem. Concr. Res. 37 (2007) 767–775. https://doi.org/10.1016/j.cemconres.2007.02.023.
[66] C. Atzeni, G. Pia, U. Sanna, N. Spanu, A fuzzy model for classifying mechanical properties of vesicular basalt used in prehistoric buildings, Mater. Charact. 59 (2008) 606–612. https://doi.org/10.1016/j.matchar.2007.05.001.
[67] A.K. Patra, S. Ramanathan, D. Sen, S. Mazumder, SANS study of fractal microstructure and pore morphology in porous titania, J. Alloys Compd. 397 (2005) 300–305. https://doi.org/10.1016/j.jallcom.2005.01.037.
[68] D. Sanyal, P. Ramachandrarao, O.P. Gupta, A fractal description of transport phenomena in dendritic porous network, Chem. Eng. Sci. 61 (2006) 307–315. https://doi.org/10.1016/j.ces.2005.06.005.
[69] J. Wu, B. Yu, A fractal resistance model for flow through porous media, Int. J. Heat Mass Transf. 50 (2007) 3925–3932. https://doi.org/10.1016/j.ijheatmasstransfer.2007.02.009.
[70] M. Yun, B. Yu, J. Cai, A fractal model for the starting pressure gradient for Bingham fluids in porous media, Int. J. Heat Mass Transf. 51 (2008) 1402–1408. https://doi.org/10.1016/j.ijheatmasstransfer.2007.11.016.
[71] P. Xu, B. Yu, Developing a new form of permeability and Kozeny–Carman constant for homogeneous porous media by means of fractal geometry, Adv. Water Resour. 31 (2008) 74–81. https://doi.org/10.1016/j.advwatres.2007.06.003.
[72] M. Yun, B. Yu, J. Cai, Analysis of seepage characters in fractal porous media, Int. J. Heat Mass Transf. 52 (2009) 3272–3278. https://doi.org/10.1016/j.ijheatmasstransfer.2009.01.024.
[73] J. Cai, B. Yu, M. Zou, M. Mei, Fractal analysis of invasion depth of extraneous fluids in porous media, Chem. Eng. Sci. 65 (2010) 5178–5186. https://doi.org/10.1016/j.ces.2010.06.013.
[74] S. Wang, B. Yu, A fractal model for the starting pressure gradient for Bingham fluids in porous media embedded with fractal-like tree networks, Int. J. Heat Mass Transf. 54 (2011) 4491–4494. https://doi.org/10.1016/j.ijheatmasstransfer.2011.06.031.
[75] H.P. Tang, J.Z. Wang, J.L. Zhu, Q.B. Ao, J.Y. Wang, B.J. Yang, Y.N. Li, Fractal dimension of pore-structure of porous metal materials made by stainless steel powder, Powder Technol. 217 (2012) 383–387. https://doi.org/10.1016/j.powtec.2011.10.053.
[76] J.J.M. Buiting, E. a. Clerke, Permeability from Porosimetry Measurements, Derivation for a Tortuous and Fractal Tubular Bundle, J. Pet. Sci. Eng. (2013) 1–12. https://doi.org/10.1016/j.petrol.2013.04.016.
[77] G. Pia, U. Sanna, Intermingled fractal units model and electrical equivalence fractal approach for prediction of thermal conductivity of porous materials, Appl. Therm. Eng. 61 (2013) 186–192. https://doi.org/10.1016/j.applthermaleng.2013.07.031.
[78] G. Pia, U. Sanna, An intermingled fractal units model to evaluate pore size distribution influence on thermal conductivity values in porous materials, Appl. Therm. Eng. 65 (2014) 330–336. https://doi.org/10.1016/j.applthermaleng.2014.01.037.
[79] G. Pia, L. Casnedi, U. Sanna, Porous ceramic materials by pore-forming agent method: An intermingled fractal units analysis and procedure to predict thermal conductivity, Ceram. Int. 41 (2015) 6350–6357. https://doi.org/10.1016/j.ceramint.2015.01.069.
[80] T. Miao, S. Cheng, A. Chen, B. Yu, Analysis of axial thermal conductivity of dual-porosity fractal porous media with random fractures, Int. J. Heat Mass Transf. 102 (2016) 884–890. https://doi.org/10.1016/j.ijheatmasstransfer.2016.06.048.
[81] Z. Deng, X. Liu, C. Zhang, Y. Huang, Y. Chen, Melting behaviors of PCM in porous metal foam characterized by fractal geometry, Int. J. Heat Mass Transf. 113 (2017) 1031–1042. https://doi.org/10.1016/j.ijheatmasstransfer.2017.05.126.

[82] Y. Wang, C. Ma, Y. Liu, D. Wang, J. Liu, A model for the effective thermal conductivity of moist porous building materials based on fractal theory, Int. J. Heat Mass Transf. 125 (2018) 387–399. https://doi.org/10.1016/j.ijheatmasstransfer.2018.04.063.
[83] X. Qin, J. Cai, P. Xu, S. Dai, Q. Gan, A fractal model of effective thermal conductivity for porous media with various liquid saturation, Int. J. Heat Mass Transf. 128 (2019) 1149–1156. https://doi.org/10.1016/j.ijheatmasstransfer.2018.09.072.
[84] X. Qin, J. Cai, Y. Zhou, Z. Kang, Lattice Boltzmann simulation and fractal analysis of effective thermal conductivity in porous media, Appl. Therm. Eng. 180 (2020) 115562. https://doi.org/10.1016/j.applthermaleng.2020.115562.
[85] H. Yu, H. Zhang, P. Buahom, J. Liu, X. Xia, C.B. Park, Prediction of thermal conductivity of micro/nano porous dielectric materials: Theoretical model and impact factors, Energy. 233 (2021) 121140. https://doi.org/10.1016/j.energy.2021.121140.
[86] D.A. Wood, Techniques used to calculate shale fractal dimensions involve uncertainties and imprecisions that require more careful consideration, Adv. Geo-Energy Res. 5 (2021) 153–165. https://doi.org/10.46690/ager.2021.02.05.
[87] S.J. Gregg, K.S.W. Sing, Adsorption, surface area and porosity: Second edition, (1982)¸1-313.
[88] A. Neimark, A new approach to the determination of the surface fractal dimension of porous solids, Phys. A Stat. Mech. Its Appl. 191 (1992) 258–262. https://doi.org/10.1016/0378-4371(92)90536-Y.
[89] F. Wang, S. Li, Determination of the Surface Fractal Dimension for Porous Media by Capillary Condensation, Ind. Eng. Chem. Res. 36 (1997) 1598–1602. https://doi.org/10.1021/ie960555w.
[90] C.T. Hsu, P. Cheng, K.W. Wong, A Lumped-Parameter Model for Stagnant Thermal Conductivity of Spatially Periodic Porous Media, J. Heat Transfer. 117 (1995) 264–269. https://doi.org/10.1115/1.2822515.
[91] B. Yu, P. Cheng, Fractal models for the effective thermal conductivity of bidispersed porous media, J. Thermophys. Heat Transf. 16 (2002) 22–29. https://doi.org/10.2514/2.6669.
[92] F. Surma, Y. Geraud, Porosity and Thermal Conductivity of the Soultz-sous-Forêts Granite, Pure Appl. Geophys. 160 (2003) 1125–1136. https://doi.org/10.1007/PL00012564.